J. Fluid Mech. (1993), *vol.* 246, *pp.* 301–320

On the transient motion of ordered suspensions of liquid drops

By C. POZRIKIDIS

Department of Applied Mechanics and Engineering Sciences, University of California at San Diego, La Jolla, CA 92093-0411, USA

(Received 24 March 1992 and in revised form 10 June 1992)

The transient motion of ordered suspensions of liquid drops, initially arranged on a cubic lattice, is studied as a model of suspension rheology. An asymptotic three-term expansion for the effective stress tensor of a dilute suspension of spherical drops is derived based on the Faxén law for the stresslet. Comparisons with available exact results for cubic lattices suggests that the expansion is remarkably accurate even at concentrations close to maximum packing. The behaviour of suspensions with recurrent structure evolving under the influence of a simple shear flow is investigated, and the results show that the time-averaged behaviour may differ substantially from the instantaneous behaviour. Transient normal stress differences may vanish in the mean, but make appreciable contributions to the instantaneous dynamics. The effect of particle deformation is assessed by numerically computing the motion of initially spherical drops arranged on a cubic lattice. At large times, the suspension is shown to exhibit periodic motions in which the drops oscillate about a mean shape with a phase shift which depends on the geometry of the lattice and the physical properties of the fluids. It is shown that drop deformations cause shear thinning and some type of elastic behaviour, and may lower the effective viscosity of the suspension below that corresponding to the dilute limit.

1. Introduction

Lattices of rigid and flexible particles provide us with useful models for studying the flow through granular media including porous rocks and fluidized beds, and the rheology of concentrated suspensions and emulsions. Their advantages are that uncertainties regarding spatial particle distributions are removed, albeit in an artificial manner, divergent infinite sums that represent interactions among an infinite number of suspended particles are bypassed, and the analysis may be conducted in a rigorous and accurate manner (Acrivos & Chang 1987). Their most serious shortcoming is geometrical idealization, but in view of the difficulty of the problem in its general statement, this may be regarded as an affordable simplification. From a more general perspective, lattice models may be viewed as standard reference configurations which allow us to assess the effect of the microstructure and to study the interplay between particle motions, particle deformations, and interparticle hydrodynamic interactions.

To appreciate the extent to which lattice models have helped us understand and describe particulate flows, it is helpful to categorize previous investigations into three general groups that include studies of (*a*) flows past fixed beds of particles emulating ordered porous media, (*b*) flows due to arrays of particles moving under the influence of a specified force or torque field with applications in particle

sedimentation and, (c) flows past arrays of freely suspended particles with applications in suspension rheology. There is a large body of literature on these topics and seminal contributions were made, among others, by Hasimoto (1959) who studied streaming flow past fixed arrays of small spherical particles and suggested relations between the void fraction and permeability, Saffman (1973) who considered flow past regular and random arrays of fixed or sedimenting particles, and Zick & Homsy (1982) and Sangani & Acrivos (1982) who computed flows past regular arrays of spherical particles of finite size. Nitsche & Brenner (1989) present a comprehensive review of studies of flow through spatially periodic arrangements of particles representing ordered porous media, and discuss the relations between the macroscopic variables and the micromechanics of the flow. Recently, two-dimensional lattices of particles were used as models for studying the behaviour of interfaces populated by surfactants (Edwards & Wasan 1991).

Focusing on our topic of interest, we consider studies of ordered suspensions of solid and liquid particles. The instantaneous behaviour of suspensions of force-free, torque-free, and spinning spherical particles arranged on cubic lattices was studied first by Kapral & Bedeaux (1978), and later in more detail in a tetralogy of papers by Adler & Brenner (1985), Adler, Zuzovski & Brenner (1985), Zuzovski, Adler & Brenner (1983), and Adler (1984). Their computations provided asymptotic expansions for the instantaneous effective stress tensor in the limit of small volume fractions. Nunan & Keller (1984) extended the results to moderate and large volume fractions, and showed that the instantaneous effective stress tensor may be expressed in terms of a rank-four viscosity tensor which involves two scalar constants. Brady *et al.* (1988) carried out additional computations to benchmark their Stokesian dynamics method, and Phan-Tien, Tran-Cong & Graham (1991) considered cubic lattices of spheroidal and cubic particles, as well as clusters of spheres. Sangani (1987) and Sangani & Lu (1987) considered cubic lattices of spherical liquid drops of arbitrary viscosity, and computed the sedimentation velocity and the instantaneous effective viscosity tensor from the dilute limit to maximum packing. Hurd *et al.* (1985) computed friction factors for lattices of charged Brownian spheres representing colloidal crystals.

Studies of instantaneous motions with preassigned structure are quite useful for illustrating the effect of the microstructure and the importance of particle constitution but, evidently, they are unable to provide information on the dynamics of a flow. This limitation is underlined by the notion that, on a macroscopic level, the motion of a suspension is properly described in terms of the time-average behaviour over a period of time which is long enough compared to the timescale of the evolution of the microstructure, but short enough to allow the meaningful computation of time averages. In the fortunate case where the suspension recovers its initial structure after a finite or even infinite amount of time, the calculation of the time averages may be effected simply by integrating the instantaneous variables over one period of the motion, whereas in the more general case where the structure of the suspension is not recurrent, the calculation of the time-average behaviour is more subtle. Adler *et al.* (1985) present a general discussion of the macroscopic averaged behaviour of ordered suspensions executing periodic motions. In any case, it is now well established that transient effects are important, and the time-average behaviour will be substantially different from the instantaneous behaviour that pertains to a particular type of lattice at a particular instant in time.

The first explicit calculation of the time-average behaviour of an ordered suspension with recurrent structure is due to Wang & Cheau (1990). These authors

considered the sliding motion of particle layers belonging to a rectangular lattice and moving under the influence of a simple shearing flow, in the limit of high concentrations. Noting that particle interactions are effected primarily through lubrication forces, and integrating the dominant component of the particle stress tensor, these authors demonstrated that the asymptotic behaviour in the limit of maximum packing is correctly captured by an earlier model due to Frankel & Acrivos (1967), in spite of previous scepticism by Marucci & Denn (1985).

Additional considerations arise when the suspended particles are allowed to deform. Flexible particles arranged on a lattice with evolve under the influence of both the straining component of the incident flow and the flow produced by particle interactions, and the magnitude and type of deformations will depend upon the particle constitution. The rate of particle deformation will involve a characteristic timescale which depends on the physical properties of the particles and the mean strain rate of the incident flow, and thus it will be a function of the ratio of viscosities of the dispersed and suspending fluid, as well as the capillary number. Particle deformations in dilute emulsions are known to be responsible for shear-thinning and elastic behaviour, and similar effects are to be expected in dense and concentrated suspensions.

It is possible, but not quite certain, that when an ordered suspension executes periodic motion, the suspended deformable particles will undergo concomitant periodic deformations due to the unsteady straining field associated with the flow due to all other particles in the lattice. In this case, the amplitude of the periodic component of the particle deformation will depend upon the relative magnitude of the timescale of particle deformation and the period of lattice motion. Since, however, the particle deformation is a nonlinear function of the local velocity field, which plays the role of a forcing function, it is plausible that the particle deformation may not observe the temporal periodicity of the lattice, and may exhibit aperiodic or even random behaviour. Numerical computations accounting for finite particle deformations are necessary to delineate this behaviour.

In this work we study the evolution of a suspension of spherical liquid drops which are initially arranged on a three-dimensional lattice, with main objectives to compare the instantaneous with the time-average behaviour, to illustrate the precise effect of particle deformations, and to establish the asymptotic behaviour at large times. As a prototypical configuration, we consider a suspension of spherical drops initially arranged on a cubic lattice and executing periodic motion under the influence of a simple shear flow.

We begin our investigation by developing an asymptotic expansion for the effective stress tensor of a suspension of spherical drops in the limit of small volume fractions. Our procedures involve the combined application of the method of reflections and Faxén's law for the stresslet. The calculations are accelerated by the use of the Ewald summation technique for obtaining the flow due to a lattice of point force dipoles and potential quadruples. When improved using rational approximations, the three-term asymptotic expansion is shown to be remarkably accurate even at volume fractions close to maximum packing. Special cases of the asymptotic expansions were developed previously by Zuzovski *et al.* (1983) and Sangani & Lu (1987) using different procedures, and our formulation generalizes their results and points out some discrepancies. Our asymptotic expansion is used to obtain estimates of the instantaneous and the time-average rheological behaviour, and to assess the effect of lattice structure.

To investigate the effect of particle deformations, in the second part of our studies

we compute the transient motion of a simple cubic lattice of spherical liquid drops. The computations rely on numerical solutions that are based on a boundary integral method. The numerical implementation involves several novel features, some of which are specific to our particular problem, but others make more general contributions. Briefly, we introduce a global description of the drop surface in terms of polar surface variables, we develop an efficient method for computing the mean curvature of the interface, and use a modified Green's function in order to reduce the cost of the computations. We conclude in §4 by discussing our results within the more general framework of suspension rheology.

2. Spherical drops at low volume fractions

We consider a linear flow $\boldsymbol{u}^{\mathrm{LIN}} = \boldsymbol{A}\cdot\boldsymbol{x}$ past a three-dimensional lattice of force-free and torque-free spherical drops of radius a and viscosity $\lambda\mu$ suspended in a fluid of viscosity μ. The instantaneous structure of the lattice is described in terms of three time-dependent base vectors $\boldsymbol{a}_1$, $\boldsymbol{a}_2$, and $\boldsymbol{a}_3$ so that the position of the lth lattice point, which coincides with the centre of a drop, is given by

$$\boldsymbol{X}_l = i_1\boldsymbol{a}_1 + i_2\boldsymbol{a}_2 + i_3\boldsymbol{a}_3, \tag{2.1}$$

where i_1, i_2, i_3 are three integers. We assume that the Reynolds number of the flow both inside and outside the drops is sufficiently small so that the motion is governed by the equations of creeping flow. We stipulate that the velocity is continuous across the boundary of each drop, but allow the surface force to undergo a discontinuity in the normal direction due to surface tension. We acknowledge that the incident flow will cause the drops to deform, but assume that the surface tension is strong enough for the drops to maintain the spherical shape. The arrangement of the drops generates a disturbance flow which observes the periodicity of the lattice. Our present objective is to assess the contribution of this flow to the effective stress tensor of the suspension in the limit of small concentrations.

We argue that when the drops are well separated, they respond to the incident flow as if they were immersed in an infinite ambient fluid. Thus, they rotate at an angular velocity which is equal to twice the vorticity of the incident flow, and generate a disturbance flow in response to the straining component of the incident flow, given by

$$u_i^{\mathrm{D}} = \mathscr{D}_{ijk}^{\mathrm{L}} d_{jk} + \mathscr{Q}_{ijk}^{\mathrm{L}} q_{jk}, \tag{2.2}$$

where $\mathscr{D}^{\mathrm{L}}$ and $\mathscr{Q}^{\mathrm{L}}$ are periodic singularities representing the flow due to a lattice of point-force dipoles and potential quadruples, respectively. The coefficients of the singularities are given by

$$\boldsymbol{d} = -\tfrac{5}{6}\gamma a^3\boldsymbol{E}, \quad \boldsymbol{q} = \tfrac{1}{6}\delta a^5\boldsymbol{E}, \tag{2.3}$$

where

$$\gamma = (\lambda+\tfrac{2}{5})/(\lambda+1), \quad \delta = \lambda/(\lambda+1) \tag{2.4}$$

and $\boldsymbol{E}$ is the symmetric component of $\boldsymbol{A}$, that is, the rate of deformation tensor of the incident flow (Pozrikidis 1992, chap. 7). The coefficients γ and δ in (2.4) were defined so that when the drops become solid particles, in which case $\lambda = \infty$, their value will reduce to one, $\gamma = \delta = 1$. Noting that $\mathscr{Q}^{\mathrm{L}} = -\frac{1}{2}\nabla^2\mathscr{D}^{\mathrm{L}}$, and using (2.3) we write (2.2) in the equivalent form

$$u_i^{\mathrm{D}} = -\tfrac{1}{6}a^3(5\gamma + \delta\tfrac{1}{2}a^2\nabla^2)\,\mathscr{D}_{ijk}^{\mathrm{L}} E_{jk}, \tag{2.5}$$

where the superscript D stands for disturbance.

Kim & Lu (1987) explain that the singularity representation (2.5) may be used to derive Faxén's law for the stresslet $\boldsymbol{S}$. We find that for a drop which is immersed in the incident flow $\boldsymbol{u}^\infty$, the stresslet is given by

$$\boldsymbol{S} = \tfrac{4}{3}\pi\mu a^3(5\gamma + \delta\tfrac{1}{2}a^2\nabla^2)\,\boldsymbol{E}^\infty, \tag{2.6}$$

where $\boldsymbol{E}^\infty$ is the rate-of-deformation tensor of the incident flow. Equation (2.6) was originally derived by Rallison (1978) using a different method. Applying (2.6) for the incident flow yields the well-known stresslet for a solitary drop,

$$\boldsymbol{S}^\infty = -8\pi\boldsymbol{d} = \tfrac{20}{3}\pi\mu a^3\gamma\boldsymbol{E}, \tag{2.7}$$

first computed by Taylor (1932), where $\boldsymbol{d}$ is given in (2.3).

We proceed next to compute the stresslet on each drop due to the disturbance flow (2.5). Following the standard method of reflections, we consider the flow in the neighbourhood of one selected drop due to all other drops in the lattice, given by (2.5). The corresponding rate of deformation tensor may be expressed in the form

$$E^{\mathrm{D}}_{ij} = -\tfrac{1}{6}a^3(5\gamma + \delta\tfrac{1}{2}a^2\nabla^2)\,\mathscr{E}^{\mathrm{DIPOLE}}_{ijmn}E_{mn}, \tag{2.8}$$

where $\mathscr{E}^{\mathrm{DIPOLE}}$ is the rate-of-deformation tensor corresponding to the singularity $\mathscr{D}^{\mathrm{L}}$. Substituting $\boldsymbol{E}^{\mathrm{D}}$ in place of $\boldsymbol{E}^\infty$ in (2.6), we obtain the leading-order correction to the stresslet

$$S^{\mathrm{D}}_{ij} = -\tfrac{2}{9}\pi\mu a^6(5\gamma + \delta\tfrac{1}{2}a^2\nabla^2)\,(5\gamma + \delta\tfrac{1}{2}a^2\nabla^2)\,\mathscr{E}^{\mathrm{DIPOLE}}_{ijmn}E_{mn}, \tag{2.9}$$

where it is reckoned that the singular contribution of the right-hand side is discarded. It is consistent to cross-out terms containing powers of a beyond the eighth, obtaining the simplified expression

$$S^{\mathrm{D}}_{ij} = -\tfrac{10}{9}\pi\mu a^6\gamma(5\gamma + \delta a^2\nabla^2)\,\mathscr{E}^{\mathrm{DIPOLE}}_{ijmn}E_{mn}, \tag{2.10}$$

where the right-hand side is evaluated at the centre of a drop after the singular contributions have been discarded. Adding (2.7) to (2.10) we derive an asymptotic expansion for the stresslet:

$$S^\infty_{ij} + S^{\mathrm{D}}_{ij} = 5\mu V_D D^{\mathrm{LIN}}_{ij} - \tfrac{5}{2}\mu V_{\mathrm{D}}^2\,\gamma\left(\frac{5}{4\pi}\gamma + V_{\mathrm{D}}^{\frac{2}{3}}\left(\frac{3}{4\pi}\right)^{\frac{5}{3}}\delta\nabla^2\right)\mathscr{E}^{\mathrm{DIPOLE}}_{ijmn}E_{mn}. \tag{2.11}$$

Based on (2.11) we find that the particle stress tensor is given by

$$\Sigma_{ij} = \tfrac{5}{2}\mu\phi\gamma\left[\delta_{im}\,\delta_{jn} - \phi\gamma\frac{5}{8\pi}\tau\mathscr{E}^{\mathrm{DIPOLE}}_{ijmn} + \phi^{\frac{5}{3}}\delta\frac{1}{3}\left(\frac{3}{4\pi}\right)^{\frac{5}{3}}\tau^{\frac{5}{3}}\mathscr{E}^{\mathrm{POT.QUADR}}_{ijmn}\right]2E_{mn}, \tag{2.12}$$

where τ is the volume of one cell, $\phi = V_{\mathrm{D}}/\tau$ is the volume fraction of the drops in the suspension, and $\mathscr{E}^{\mathrm{POT.QUADR}}$ is the rate-of-deformation tensor corresponding to the singularity $\mathscr{Q}^{\mathrm{L}}$. The effective stress tensor of the suspension is given by

$$\sigma^{\mathrm{EFF}}_{ij} = \mu^{\mathrm{EFF}}_{ijmn}\,2E_{mn}, \tag{2.13}$$

where

$$\mu^{\mathrm{EFF}}_{ijmn} = \mu\delta_{im}\,\delta_{jn} + \tfrac{5}{2}\mu\phi\gamma\left[\delta_{im}\,\delta_{jn} - \phi\gamma\frac{5}{8\pi}\tau\mathscr{E}^{\mathrm{DIPOLE}}_{ijmn} + \phi^{\frac{5}{3}}\delta\frac{1}{3}\left(\frac{3}{4\pi}\right)^{\frac{5}{3}}\tau^{\frac{5}{3}}\mathscr{E}^{\mathrm{POT.QUADR}}_{ijmn}\right] \tag{2.14}$$

is the rank-four effective viscosity tensor.

In order to compute the rate-of-deformation tensors $\mathscr{E}^{\mathrm{DIPOLE}}$ and $\mathscr{E}^{\mathrm{POT.QUADR}}$ on the right-hand side of (2.12) we require an efficient method for obtaining the velocity

field due to a three-dimensional array of point force dipoles and potential quadruples, represented by $\mathscr{D}^{\mathrm{L}}$ and $\mathscr{Q}^{\mathrm{L}}$, but this is provided by the Ewald summation technique developed by Beenaker (1986) and discussed in detail in Appendix A.

2.1. *Cubic lattices*

We proceed to consider instantaneous configurations in which the particles are arranged on a cubic lattice, with a main objective to compare our asymptotic results with those derived by previous numerical and asymptotic analyses. The base vectors of the lattices are $(1,0,0)$, $(0,1,0)$, $(0,0,1)$ for the simple cubic lattice, $(1,1,-1)$, $(-1,1,1)$, $(1,-1,1)$ for the body-centred cubic lattice, and $(1,1,0)$, $(0,1,1)$, $(1,0,1)$ for the face-centred cubic lattice.

Zuzovski *et al.* (1983) noted that the behaviour of a suspension of solid spherical particles arranged on a cubic lattice in a general linear flow may be deduced from the behaviour in a purely straining flow with $\boldsymbol{A} = \frac{1}{2}(k, -k, 0)$ and a simple shear flow with $\boldsymbol{A} = (k, 0, 0)$, where k is the shear rate. Nunan & Keller (1984) showed that the effective stress tensor of a suspension of solid spherical particles is given by

$$\sigma_{ij}^{\mathrm{EFF}} = \mu_{ijmn}^{*} 2A_{mn}, \tag{2.15}$$

where

$$\mu_{ijmn}^{*} = \mu(1+\beta)\tfrac{1}{2}(\delta_{im}\delta_{jn}+\delta_{in}\delta_{jm}-\tfrac{2}{3}\delta_{ij}\delta_{mn})+\mu(\alpha-\beta)(\delta_{ijmn}-\tfrac{1}{3}\delta_{ij}\delta_{mn}). \tag{2.16}$$

The matrix δ_{ijmn} is equal to one if all indices are identical, and is equal to zero otherwise. It will be noted that μ^{*} is characterized by the two scalar coefficients α and β which depend upon the particle concentration, ϕ, and the geometry of the lattice. The values of these constants may be found by studying the behaviour of the suspension in a purely straining and a simple shear flow. Further, Nunan & Keller noted that, in all cases, the spheres rotate at an angular velocity which is equal to twice the vorticity of the incident flow, independently of the volume fraction. Physically, this behaviour may be understood by noting that, owing to the symmetries of the cubic lattice configuration, the flow generated in the vicinity of one individual particle due to all other particles is a purely straining flow, and thus it does not induce rotation. Sangani & Lu (1987) indicated that (2.15) and (2.16) remain valid for spherical drops of arbitrary viscosity.

Considering the modular cases of purely straining and simple shear flow, we non-dimensionalize all variables using as characteristic lengthscale the length of the cubical cell $L = (\tau)^{\frac{1}{3}}$, as characteristic timescale $1/k$, and as characteristic stress scale μk. Using (2.12) we find that the particle stress tensor is given by $\boldsymbol{\Sigma} = \alpha 2\boldsymbol{E}$ and $\boldsymbol{\Sigma} = \beta 2\boldsymbol{E}$, for the simple shear and purely straining flow, respectively. The coefficients α and β are given by the asymptotic expansions

$$\alpha = \tfrac{5}{2}\gamma\phi(1-\phi\gamma\alpha_1+\phi^{\frac{5}{3}}\delta\alpha_2+\ldots), \quad \beta = \tfrac{5}{2}\gamma\phi(1-\phi\gamma\beta_1+\phi^{\frac{5}{3}}\delta\beta_2+\ldots). \tag{2.17}$$

It is worth noting that in the special case of inviscid bubbles, $\lambda = 0$, $\delta = 0$, the third-order correction vanishes.

In order to improve the accuracy of (2.17), we use the theory of rational or Padé approximations and introduce the equivalent expansions

$$\alpha = \tfrac{5}{2}\gamma\phi(1+\phi\gamma\alpha_1-\phi^{\frac{5}{3}}\delta\alpha_2+\ldots)^{-1}, \quad \beta = \tfrac{5}{2}\gamma\phi(1+\phi\gamma\beta_1-\phi^{\frac{5}{3}}\delta\beta_2+\ldots)^{-1}. \tag{2.18}$$

Analogous expansions were derived previously by Zuzovski *et al.* (1983) for the special case of solid particles, i.e. $\gamma = \delta = 1$, and by Sangani & Lu (1987) up to second order for the more general case of drops with arbitrary viscosity. The generalization of (2.18) to liquid drops and the interpretation of the coefficients in terms of periodic

	α_1	α_2	β_1	β_2
Simple cubic	−3.7870	−3.4267	0.8580	2.2845
Body-centred cubic	−0.1408	1.0788	−1.5728	−0.7192
Face-centred cubic	−0.2361	0.8232	−1.5093	−0.5488

TABLE 1. The expansion coefficients defined in (2.18) for cubic lattices

χ	α(2−exp)	α(3−exp)	α(exact)	β(2−exp)	β(3−exp)	β(exact)
0.5	0.1386	0.1356	0.1356	0.1102	0.1115	0.1115
0.6	0.2827	0.2655	0.2657	0.1853	0.1907	0.1908
0.7	0.6000	0.5054	0.5076	0.2837	0.3015	0.3019
0.8	1.6215	0.9768	0.9975	0.4041	0.4539	0.4557
0.9	−56.33	2.0103	2.244	0.5434	0.6681	0.6738
1.0	−2.361	4.7043	<7.70	0.6971	0.9900	1.003

TABLE 2. Comparison between approximate and exact values of α and β for the simple cubic lattice and $\lambda = 1$; χ is the ratio of the drop radius to the drop radius at maximum packing. 2−exp and 3−exp denote the predictions of (2.18) maintaining respectively two and three terms

singularities is a new contribution. To this end we note that the improved expansion (2.18) could have been obtained in a direct manner and without any further approximations if the asymptotic procedure of Zuzovski *et al.* (1983) was used. This observation provides us with a physical premise for rewriting (2.17) in the form of (2.18), and furnishes a mathematical justification beyond that underlying the standard theory of Padé approximants (Hinch 1991, p. 151).

In table 1 we tabulate the values of the coefficients α_1, α_2, β_1, and β_2 computed using our numerical procedures. Most of these results are in perfect agreement with those reported by Zuzovski *et al.* (1983) and Sangani & Lu (1987). There are occasional discrepancies in the third decimal place, by one or two units, and a more serious disagreement in the second decimal place for the value of β_1 for the simple cubic lattice. Curiously, Zuzovski *et al.* and Sangani & Lu also disagree about this value, suggesting −0.862 and −0.814, respectively. In any case, it is safe to argue that these rather minor discrepancies are due to numerical inaccuracies.

We turn next to evaluate the accuracy of the asymptotic expansions (2.18). Sangani & Lu (1987) provide tables and graphs of exact values of α and β for a simple cubic lattice in a range of viscosity ratios λ and volume fractions up to maximum packing $\phi_{\max} = \frac{1}{6}\pi$. Their results are presented in terms of the ratio of the drop radius to the radius at maximum packing, $\chi = (\phi/\phi_{\max})^{\frac{1}{3}}$. Comparing our results with those reported by Sangani & Lu we find remarkable agreement at low and moderate values of χ. For instance, for $\chi = 0.70$ we find that the predictions of (2.18) agree with the exact values up to the third, and occasionally up to the fourth, significant figure. An exception is the value of β for $\lambda = 0$ where we observe disagreement at the first significant figure. The source of this discrepancy could not be identified. The agreement worsens at higher values of χ, but the error remains within reasonable bounds.

To illustrate the range of accuracy of our asymptotic expansion, in table 2 we present values of α and β for a simple cubic lattice with $\lambda = 1$ in a range of moderate and high radii ratio χ, including the predictions of the expansion (2.18) maintaining two or three terms, and the exact values provided by Sangani & Lu (1987). We observe that the two-term expansion is remarkably accurate up to $\chi = 0.50$, and the

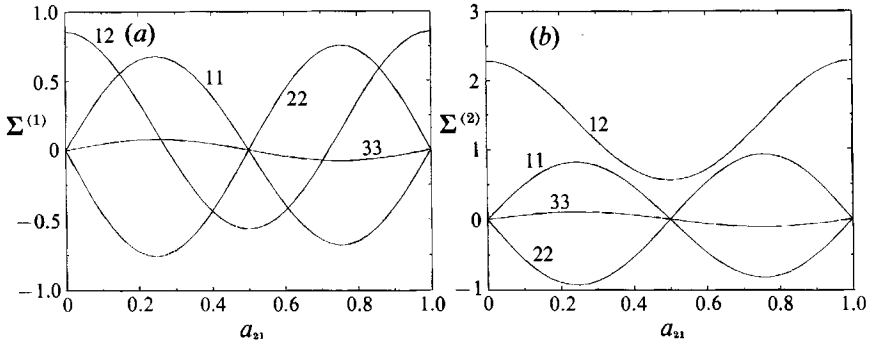

FIGURE 1. The stress tensors (*a*) $\mathbf{\Sigma}^{(1)}$ and (*b*) $\mathbf{\Sigma}^{(2)}$, for the simple cubic lattice.

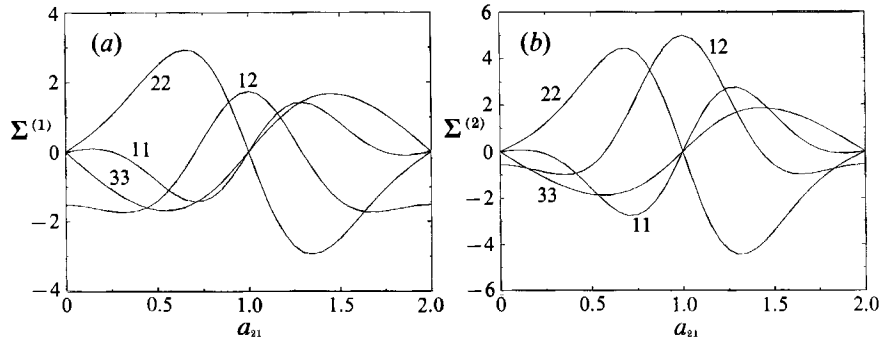

FIGURE 2. The stress tensors (*a*) $\mathbf{\Sigma}^{(1)}$ and (*b*) $\mathbf{\Sigma}^{(2)}$, for the body-centred cubic lattice.

three-term expansion is surprisingly accurate up to $\chi = 0.90$. These comparisons make us confident that our results on transient behaviour, discussed below, will be quite accurate at moderate and even larger volume fractions close to maximum packing.

One important feature of table 2 is that the effect of particle interactions on the effective stress tensor becomes significant only when the particle concentration is close to maximum packing. It is interesting to observe, in particular, that the effective shear stress in a simple shearing flow is only doubled when $\chi = 1.00$, in spite of strong lubrication forces at the points of contact.

2.2. *Transient behaviour in a simple shear flow*

We proceed next to discuss the transient behaviour of cubic lattices considering, in particular, the behaviour in a simple shear flow oriented along the 1-axis. Under the influence of this flow the cubic lattices will deform but will recover their original configuration after a period which depends upon the type of the lattice. Maintaining our previous non-dimensionalization we find that the period of the motion will be equal to 1, 2, and 2, respectively, for the simple, the body-centred, and the face-centred lattice.

Equations (2.12) and (2.13) suggest that the particle stress tensor may be expressed in the form

$$\mathbf{\Sigma} = \tfrac{5}{2}\mu\phi\gamma[2\boldsymbol{E} - \phi\gamma\mathbf{\Sigma}^{(1)} + \phi^{\frac{5}{3}}\delta\mathbf{\Sigma}^{(2)}]. \tag{2.19}$$

In figures 1(*a*, *b*), 2(*a*, *b*), and 3(*a*, *b*) we plot the four non-vanishing components of $\mathbf{\Sigma}^{(1)}$ and $\mathbf{\Sigma}^{(2)}$ as functions of time over one period of the motion. The average values

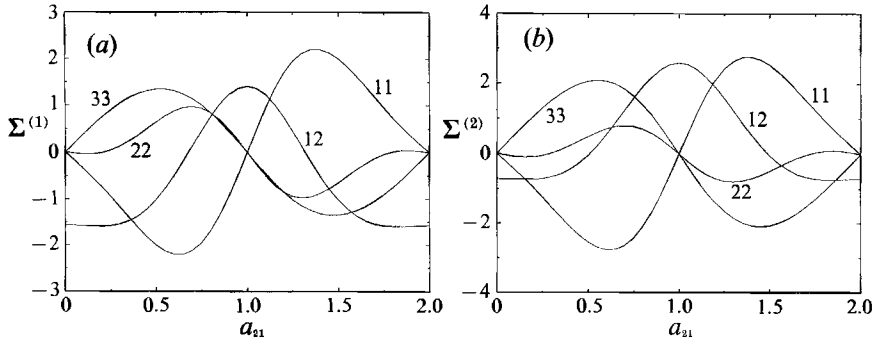

FIGURE 3. The stress tensors (*a*) $\boldsymbol{\Sigma}^{(1)}$ and (*b*) $\boldsymbol{\Sigma}^{(2)}$, for the face-centred cubic lattice.

	$\langle\beta_1\rangle$	$\langle\beta_2\rangle$
Simple cubic	0.1368	1.4030
Body-centred cubic	−0.5566	0.4419
Face-centred cubic	−0.6531	0.7872

TABLE 3. The mean values of the expansion coefficients

of all except the shearing components of $\boldsymbol{\Sigma}^{(1)}$ and $\boldsymbol{\Sigma}^{(2)}$ are equal to zero, and this implies that the macroscopic motion exhibits Newtonian behaviour with an effective shear viscosity which depends upon the structure of the lattice. The overall behaviour of the suspension, which is the one that will be recorded by an experimental apparatus operating over a sufficiently long period of time, is described by the average particle stress tensor, $\langle\boldsymbol{\Sigma}\rangle$, which is equal to the mean value of the instantaneous stress tensor over one period of motion. We find $\langle\boldsymbol{\Sigma}\rangle = \langle\beta\rangle\, 2\boldsymbol{E}$ where

$$\langle\beta\rangle = \tfrac{5}{2}\gamma\phi(1+\phi\gamma\langle\beta_1\rangle - \phi^{\frac{5}{3}}\delta\langle\beta_2\rangle)^{-1}. \tag{2.20}$$

In table 3 we present the values of $\langle\beta_1\rangle$ and $\langle\beta_2\rangle$ for the three cubic lattices. A comparison with the instantaneous values presented in table 1 reveals serious disagreements and differences in the sign, thereby confirming that the instantaneous behaviour may differ considerably from the mean behaviour. Further, the strong dependence of the mean values on the type of lattice indicates the sensitivity of the rheological behaviour of the suspension to the geometry of the microstructure. Returning to figures 1, 2, and 3, we observe that the instantaneous normal stresses and normal stress differences are of the same order of magnitude as the instantaneous shear stresses, and this implies that the suspensions will exhibit appreciable transient elastic effects.

To place our results into a more general framework, it is helpful to compare our asymptotic predictions with those furnished by previous approximate theories and empirical models. A popular type of expansion for the particle stress tensor of a random suspension of spherical particles is

$$\boldsymbol{\Sigma} = \mu\phi(\tfrac{5}{2} + k_1\phi + k_2\phi^2 + \ldots)\, 2\boldsymbol{E} \tag{2.21}$$

which is similar to our expansion (2.19), but presents a different scaling at higher orders. This variation is a reflection of the ordered and random nature of the particle arrangement. Several investigators proposed values of k_1 in the range between 7 and 14 (Zuzovsky *et al.* 1983). Equation (2.20) along with table 3 suggest the values

-0.342, 1.391, and 1.633 for the three cubic lattices. The notable differences confirm the notion that the specific geometry of the microstructure has a considerable effect on the constitutive equation of the suspension.

3. Deformable drops and finite volume fractions

The remarkable agreement between the asymptotic results and available numerical solutions for cubic lattices at moderate and large concentrations indicate that, apart from geometrical idealization, the most crucial assumption of the asymptotic analysis is that the drops maintain the spherical shape. We proceed now to relax this assumption by considering the transient motion of a simple cubic lattice of deformable drops with finite surface tension under the influence of a simple shear flow which is oriented along one side of the lattice. At the initial instant, the drops are assumed to have a spherical shape. Computational considerations force us to limit our investigations to the case $\lambda = 1$ in which the viscosity of the drop is equal to that of the suspending fluid. Studying the effect of λ in the context of a boundary integral method appears to be not feasible with the presently available computing facilities.

3.1. *Boundary integral formulation*

To compute the motion of the drops we follow the standard boundary integral formulation and decompose the velocity field into the incident velocity field, which is a simple shearing flow, and a disturbance velocity field due to the drops. Noting that the pressure drop across each cell is equal to zero, and requiring that the net flow rate is not altered by the presence of the drops, we express the disturbance flow in terms of a boundary integral over the surface of one drop involving a single-layer and a double-layer Stokes hydrodynamic potential. Restricting our attention to the case $\lambda = 1$ we obtain an integral representation of the velocity in terms of the incident velocity, and a single-layer potential whose density is equal to the discontinuity in the surface force across the interface,

$$u_j(\boldsymbol{x}_0) = u_j^{\infty}(\boldsymbol{x}_0) - \frac{1}{8\pi\mu}\int_D \Delta f_i(\boldsymbol{x})\, G_{ij}(\boldsymbol{x}, \boldsymbol{x}_0)\, \mathrm{d}S(\boldsymbol{x}), \tag{3.1}$$

where D is the surface of one drop (Pozrikidis 1992, chap. 5). The kernel $\boldsymbol{G}$ is a periodic Green's function representing the flow due to a three-dimensional lattice of point forces whose configuration is identical to that of the lattice of the drops. Hasimoto (1959) and Saffman (1973) derive explicit expression for $\boldsymbol{G}$ in terms of Fourier series (see also Appendix B).

Assuming that the interfacial tension γ is constant and the density of the drops is equal to that of the ambient fluid, we write $\Delta \boldsymbol{f} = \gamma 2\kappa \boldsymbol{n}$, where κ is the mean curvature of the interface and $\boldsymbol{n}$ is the unit vector normal to the surface of the drop pointing into the ambient fluid. Substituting this expression into (3.1), setting $\boldsymbol{u}^{\infty} = (kx_2, 0, 0)$, and non-dimensionalizing lengths by the equivalent drop radius a, the velocity by ka and the stress by μk, we obtain the dimensionless integral equation

$$u_j(\boldsymbol{x}_0) = \delta_{j1}\, x_{0,2} - \frac{1}{8\pi C}\int_D 2\kappa(\boldsymbol{x})\, n_i(\boldsymbol{x})\, G_{ij}(\boldsymbol{x}, \boldsymbol{x}_0)\, \mathrm{d}S(\boldsymbol{x}), \tag{3.2}$$

where $C = ka\mu/\gamma$ is the capillary number. It should be noted that if λ were not equal to one, the velocity field could not be obtained simply as a surface integral as in (3.2), but would have to be computed as the solution of a Fredholm integral equation of

the second kind (Pozrikidis 1992). This, however, would require a prohibitive computational cost.

The effective stress tensor of the suspension is given by $\boldsymbol{\sigma}^{\mathrm{EFF}} = 2\boldsymbol{E}^{\mathrm{EFF}} + \boldsymbol{\Sigma}$, where $\boldsymbol{E}^{\mathrm{EFF}}$ is the average rate of deformation tensor, and

$$\Sigma_{ij} = \frac{3}{4\pi}\phi \int_D \Delta f_i x_j \, \mathrm{d}S = \frac{3}{4\pi}\phi \frac{1}{C} \int_D 2\kappa n_i x_j \, \mathrm{d}S \tag{3.3}$$

is the particle stress tensor representing the contribution of the suspended array. The asymptotic theory of Taylor (1932), which is applicable for spherical drops at low volume fractions, predicts $\boldsymbol{\Sigma} = \frac{7}{4}\phi 2\boldsymbol{E}$. It will be noted that this expression does *not* arise from (3.3) under the assumption that the drops have a spherical shape but, instead, it must be computed as the asymptotic value of (3.3) in the limit as C tends to zero. In this limit the curvature of the drops becomes constant and the off-diagonal integrals in (3.3) have very small values which, however, are divided by C to make finite contributions.

Equation (3.2) suggests that the evolution of a drop in the array may be described by marking the interface with a grid of marker points, evaluating the velocity at the marker points, simply by computing the right-hand side of (3.2), and advancing the position of the marker points. Unfortunately, as noted by Zick & Homsy (1982) and Nunan & Keller (1984), the computation of the periodic Green's function, which is necessary for the evaluation of the single-layer integral, is prohibitively expensive. These authors were able to reduce the computational expense by expanding the density of the single-layer potential, which is an unknown in their formulations, in a series of orthogonal polynomials, and then exploiting the bi-orthogonality of the expansion of the density and that of the Green's function. Their method works well for particles of spherical shape, but is not applicable for particles with more general geometries such as deformed drops.

One way to circumvent the above difficulty is to observe that the force exerted on each drop vanishes, and then replace the exact Green's function with a modified Green's function, $\boldsymbol{G}^{\mathrm{M}}$, which represents the flow due to a collection of periodic arrays of point forces, where the total strength of the point forces over one cell is equal to zero. This modified Green's function was derived by Beenaker (1986), was used in dynamic simulations by Brady *et al.* (1988), and for completeness it is also given in Appendix B.

3.2. *Numerical procedures*

Our numerical procedure follows the standard boundary element methodology but entails several novel features. First, we take advantage of the left-and-right symmetry of the flow with respect to the (x, y)-planes, as well as the point symmetry with respect to the centre of each drop, to reduce the computational domain down to one quarter of the surface of a drop. To describe the interface we introduce two non-orthogonal surface variables ξ and η, as illustrated in figure 4. At the initial instant, we cover the interface with a grid of marker points and assign values of ξ and η at the grid points, where ξ is the polar angle θ, and η is the z-coordinate. The lines of constant ξ or η, and the corresponding tangent vectors are computed by differentiating $\boldsymbol{x}(\xi, \eta)$ using Fourier interpolations. The normal vector to the interface at the grid points is computed by taking the cross-product of the two tangent vectors.

The computation of the mean curvature is an important task which was seen to cause conceptual difficulties and numerical inaccuracies in previous computations using standard boundary element methods (Pozrikidis 1992, chap. 6). These

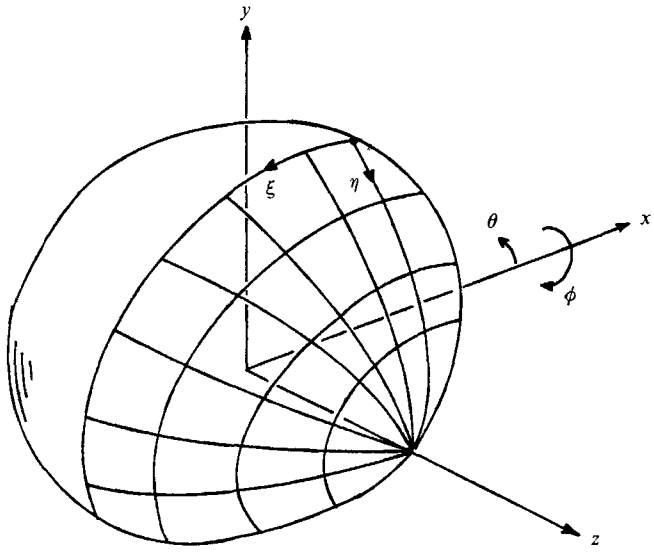

FIGURE 4. Configuration of a grid on the surface of a drop.

difficulties are attributed to the folding of the extension of the boundary elements outside the interface. In our procedures, we circumvent the explicit computation of the mean curvature by expressing the integral in (3.2) as a sum of the product of two integrals over the boundary elements, writing

$$u_j(\boldsymbol{x}_0) = C\delta_{j1}\, x_{0,2} - \frac{1}{8\pi}\sum_{n=1}^{N}\frac{1}{A_n}\int_{E_n} 2\kappa(\boldsymbol{x})\, n_i(\boldsymbol{x})\, S(\boldsymbol{x}) \int_{E_n} G_{ij}^{\mathrm{M}}(\boldsymbol{x}, \boldsymbol{x}_0)\, \mathrm{d}S(\boldsymbol{x}), \tag{3.4}$$

where E_n and A_n denote the nth boundary element and its associated surface area, and N is the total number of elements. The critical advantage of this particular discretization is that the integral of the surface force over each element may be computed as a contour integral round the perimeter of the element, as

$$\int_{E_n} 2\kappa(\boldsymbol{x})\, \boldsymbol{n}(\boldsymbol{x})\, S(\boldsymbol{x}) = \int_{C_n} \boldsymbol{n}(\boldsymbol{x}) \times \boldsymbol{t}(\boldsymbol{x})\, \mathrm{d}l(\boldsymbol{x}) \tag{3.5}$$

(Pozrikidis 1992, chap. 5). In practice, we find that applying the trapezoidal rule is sufficient for computing the contour integrals in (3.5) with reasonable accuracy, while using information about the normal vectors only at the grid points.

To compute the non-singular integral of the modified Green's function over a rectangular element in (3.4), we use a compound quadrature which involves applying three-point quadratures for each of the four plane triangles that are formed by bisecting the element using the two diagonals. To compute the singular integrals we introduce a local polar representation with origin at the singular point, designed to annihilate the singularity at the origin, and then integrate in polar coordinates using the Gauss–Legendre quadrature. Care is taken that the integration procedure preserves the inherent symmetries of the flow.

In the final stage of our numerical procedure we compute the velocity at the grid points, and advance their position with the normal component of the velocity using Euler's method. To screen out numerical instabilities, we keep the size of the time step Δt at the sufficiently low levels 0.01 or 0.02 and, in addition, after each time step, we smooth out the level ξ-curves on the interface using the five-point smoothing

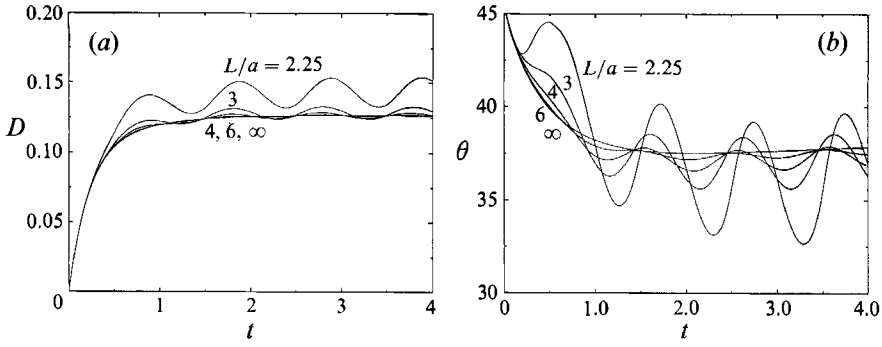

FIGURE 5. The evolution of (*a*) the drop deformation parameter D and (*b*) orientation angle θ, for $C = 0.1$ and several lattice lengths.

formula of Longuet-Higgins & Cokelet (1976). Specifically, we replace the grid point $\boldsymbol{x}_i$ with the weighted average $\frac{1}{16}(-\boldsymbol{x}_{i-2}+4\boldsymbol{x}_{i-1}+10\boldsymbol{x}_i+4\boldsymbol{x}_{i+1}-\boldsymbol{x}_{i+2})$. To this end, we remark that our global parametrization of the interface is superior to local parametrizations used in standard boundary or finite element methods, for they allow a straightforward global numerical manipulation of the interface.

Owing to numerical error, the volume of a drop was seen to decrease by a few percent from the beginning to the end of a computation. To suppress the accumulation of this error, we subjected the drops to a weak isotropic expansion after every step so that their volume is reset to the exact value. Extensive preliminary computations showed that, although small numerical differences were detected, neither grid smoothing nor expansion had a prominent effect on the behaviour of the array. The majority of our computations was performed using a 12 by 6 grid over one quarter of the interface. The computations were executed on SUN-IPC Sparcstations, and a complete computation required approximately 44 hours of CPU time. The results presented below are estimated to be 5% to 10% in error, but show the correct qualitative behaviour.

3.3. *Results and discussion*

We compute the motion of a suspension of liquid drops which, at the initial instant, are arranged on a simple cubic lattice. We consider the motion as a function of the reduced lattice length L/a and capillary number C, where L is the length of one side of the cubic cell, and a is the radius of a drop. The volume fraction of the drops is $\phi = 4\pi a^3/(3L^3)$.

In the limit as L/a tends to infinity, the drops behave as if they were immersed in an infinite ambient shear flow. Previous analyses of the behaviour of solitary drops have shown that when $\lambda = 1$, the drops deform and obtain a stationary shape as long as the capillary number C is less than roughly 0.4 (Rallison 1984). Beyond this critical value, surface tension is not able to withstand the deforming action of viscous stresses, and the drops exhibit continuous elongation and eventual breakup.

We begin by considering the effect of lattice length, keeping the capillary number constant. In figure 5(*a*, *b*) we illustrate the evolution of the deformation parameter D, and orientation angle θ, for $C = 0.1$ and lattice lengths $L/a = \infty$, 6, 4, 3, 2.25. The deformation parameter D, introduced by Taylor (1934), is defined as $D = (L-M)/(L+M)$, where L and M are maximum and minimum dimensions of the drop in the (x, y)-plane. Inspecting figure 5(*a*) we observe an initial evolution period in which the drops change from the spherical shape to an elongated shape. At later

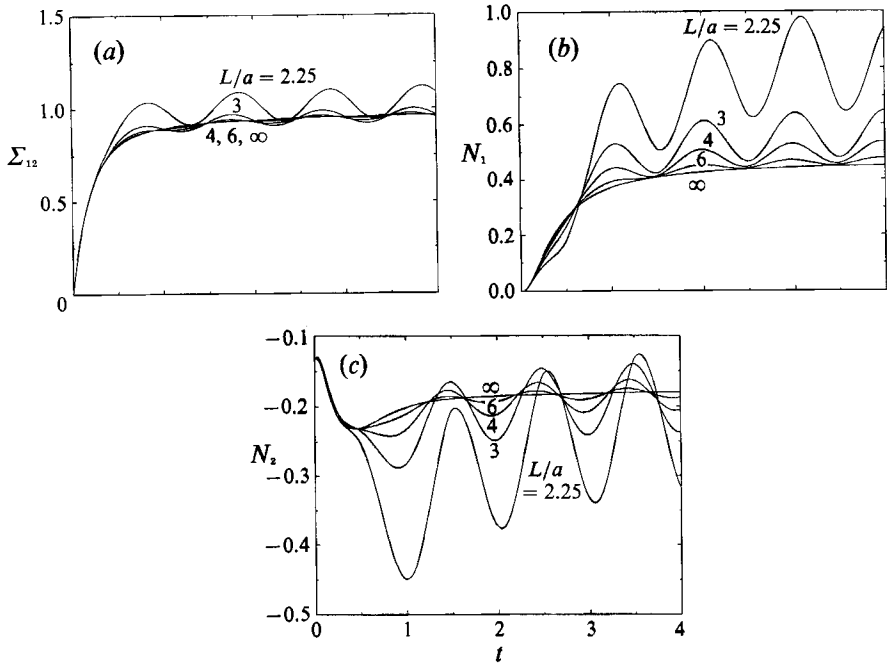

FIGURE 6. The (*a*) particle shear stress, (*b*) first normal stress difference, and (*c*) second normal stress difference, for $C = 0.1$ and several lattice lengths, normalized by $\frac{7}{4}\phi$.

times, we observe the onset of periodic motion with a period which is identical to the period of recurrence of the lattice, in which the drops deform in an oscillatory fashion in response to the periodic forcing induced by the evolving array. The amplitude of the oscillations increases as the lattice length is reduced. The phase of the oscillations and the mean value of the deformations show a weak dependence on L/a.

Turning to figure 5(*b*) we observe that the orientation angle θ undergoes an initial adjustment, and then exhibits a periodic behaviour which is characterized by oscillations about a mean value and may be described as flipping motion. The amplitude of the oscillations is more pronounced compared to that of the deformation parameter D. In all cases, the deviation of the mean value of the inclination angle from $\frac{1}{4}\pi$ is lower than, but roughly equal to, that of solitary drops corresponding to the limit $L/a = \infty$. It is interesting to note that there is a substantial phase shift between the oscillations in D and θ.

We proceed next to examine the behaviour of the particle stress tensor for the cases depicted in figure 5(*a*, *b*). In figure 6(*a*, *b*, *c*) we plot the shearing component of the particle stress tensor and the corresponding first and second normal stress differences, all normalized by the particle shear stress for a dilute suspension of spherical drops, which is equal to $\frac{7}{4}\phi$. Examining first figure 6(*a*) we observe the familiar initial transient growth and the onset of periodic behaviour. At large times, the particle shear stress exhibits strong oscillations which are nearly in phase with the deformation curves shown in figure 5(*a*). The mean amplitude of the oscillations increases as L/a is decreased, and the mean values of the particle shear stress are always less than the limiting value for a dilute suspension computed by Taylor (1932). Hydrodynamic interactions among the drops tend to increase the effective shear viscosity of the suspension, drop deformation provides a relieving mechanism, and figure 6(*a*) shows that the latter dominates the former.

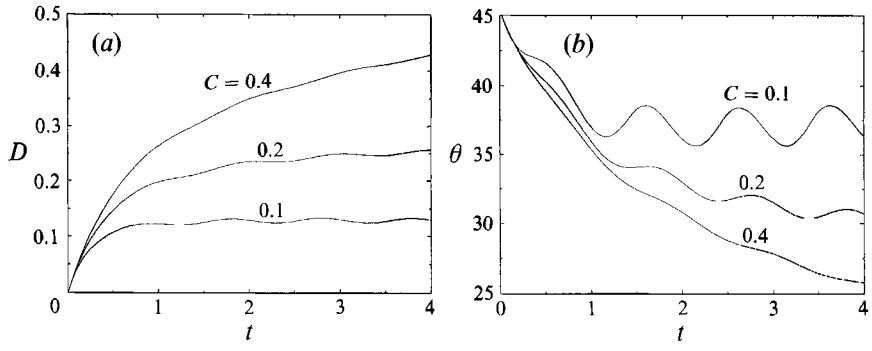

FIGURE 7. The evolution of (*a*) the drop deformation parameter D and (*b*) orientation angle θ, for $L/a = 3$ and several capillary numbers.

Inspecting figure 6(*b*, *c*) we see that the first normal stress difference is always positive, the second normal stress difference is always negative, and the magnitude of the former is clearly larger than that of the latter. At large times, the curves show the familiar periodic behaviour, and the oscillations of the first normal stress difference are nearly out of phase with those of the second normal stress difference. The mean values of the normal stress differences are substantially different than zero, indicating that the suspension exhibits some type of overall elastic behaviour. To this end, we recall that the average values of the normal stress differences of a suspension of spherical drops are equal to zero, which is in agreement with the well-established notion that drop deformability is responsible for non-Newtonian behaviour.

To illustrate the effect of drop deformability, expressed by the capillary number C, we consider the behaviour of an array with fixed lattice length $L/a = 3$ and $C = 0.1$, 0.2, 0.4. In figure 7(*a*, *b*) we plot the drop deformation parameter D and orientation angle θ from inception of the motion up to a well-established asymptotic behaviour. For $C = 0.1$, 0.2, we observe the onset of periodic motion at large times, but for $C = 0.4$ we have no indication that the drops will exhibit oscillations about a mean shape. Evidently, there is a critical capillary number, which is close to 0.4, above which the drops undergo continuous elongation and eventual breakup, just as they do in the limit of infinite dilution, for $L/a = \infty$. Owing to the degradation of the surface grid, we were not able to compute the late stages of the motion of the elongated drop for $C = 0.4$. We conclude that interparticle hydrodynamic interactions and squeezing motions between close-packed drops are not capable of maintaining compact drop shapes. It is interesting to note that the amplitude of the oscillations decreases as the drops become more flexible, which is somewhat unexpected behaviour.

The effect of drop deformation on the particle stress tensor is illustrated in figure 8(*a*–*c*). The perfect sinusoidal lines, labelled $C = 0$, represent the predictions of the asymptotic analysis for spherical drops described in the previous section. Clearly, our numerical results agree with the asymptotic results in the limit of small C or large surface tension. The magnitude of the mean particle shear stress, illustrated in figure 8(*a*), decreases appreciably as C is increased, and this is an unambiguous manifestation of shear-thinning behaviour. The behaviour of the normal stress differences, illustrated in figure 8(*b*, *c*), shows once more that the suspension exhibits some type of elastic behaviour which becomes more pronounced at larger values of C, i.e. larger drop deformations.

The above results pertain to the special case $\lambda = 1$, where the viscosity of the drops

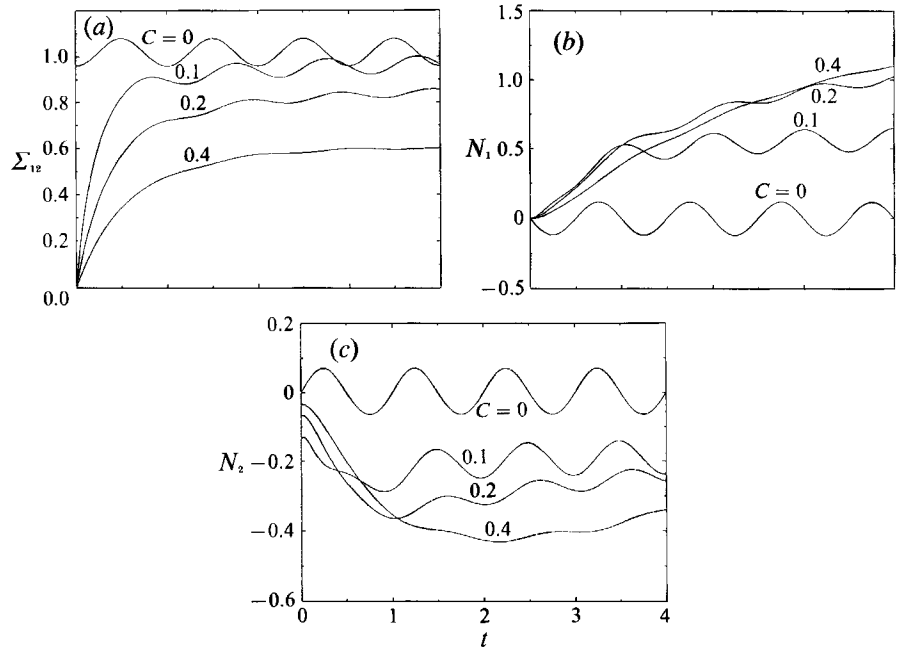

FIGURE 8. The (*a*) particle shear stress, (*b*) first normal stress difference, and (*c*) second normal stress difference, for $L/a = 3$ and several capillary numbers, normalized by $\frac{1}{4}\phi$.

is equal to that of the ambient fluid, but previous experience suggests that the main features of the motion are insensitive to the value of λ, as long as this is of order 1 or less (Rallison 1984). The behaviour of a suspension of deformable drops is expected to be significantly different at large values of λ but, unfortunately, investigations in this regime are prohibited by excessive computational cost.

4. Concluding remarks

We studied the motion of ordered suspensions of viscous drops arranged on cubic lattices, and investigated the effect of volume fraction and drop deformation. For the types of motions considered, we found that the drops deform in an oscillatory manner about a mean value, causing a corresponding oscillation of the particle stress tensor. It is now appropriate to discuss the significance of our results, and to evaluate the applicability of our conclusions within the more general framework of suspension rheology.

The ability of ordered suspensions to illustrate the behaviour of a typical suspension encountered in practice must be regarded with caution. In the first place, unless a suspension is sufficiently concentrated or electrical and colloidal forces play a dominant role, it is unlikely that hydrodynamic interactions will lead to spontaneous formation of perfect lattices, and even if they do, it is quite certain that hydrodynamic instabilities and random motions will destroy the organized flow. Evidence for spontaneous lattice formation in simple shear flows is presented by Hoffman (1972, 1974) for dense suspensions of spherical particles, Secomb, Fischer & Skalak (1983) for close-packed suspensions of red blood cells, and Ackerson & Clark (1983) and Hurd *et al.* (1985) for dilute suspensions of electrically charged particles. This behaviour, however, appear to occur exclusively in the specific case of simple

shearing flow. Under more general circumstances, the spatial particle distribution will be determined by the convective characteristics of the mean flow which is unlikely to lead to organized motion. Further, the idea of describing the flow of a random suspension in terms of the time-average behaviour of a large number of suspensions with distinct but recurrent structure is appealing but lacks a theoretical basis.

There is yet another kinematical feature that idealizes the behaviour of ordered suspensions with respect to that of a random suspension. Studies of ordered suspensions are necessarily restricted to circumstances where the motions of the particles are kinematically permissible, implying that particle collisions and anisotropic dilatations are prohibited. Unfortunately, these motions are considered to play key roles in dissipating energy, and thus in determining the effective viscosity of the fluid (Thomas 1965; Frankel & Acrivos 1967). Fortunately, for cubic lattices and for the types of motion considered in the present study, the suspensions observe the well-established asymptotic behaviour in both limits of infinite dilution and maximum packing (Taylor 1932; Wang & Cheau 1990).

We conclude that studies of ordered suspensions are not expected to provide direct information on the rheology of general dispersed systems. Instead, investigating the motion of ordered suspensions should be regarded as a means of extracting information on specific aspects of suspension rheology including the relation between the instantaneous and time-average motions, and the simultaneous effect of particle shapes, particle deformations, and interparticle interactions.

Thanks are due to Professor J. Goddard for helpful discussions and to Professor J. F. Brady for useful comments. This work is supported by the National Science Foundation, Grant CTS-9020728, the Exxon Education Foundation, and the Eastman Kodak Company.

A motion picture video of the numerical simulations is available from the author on request.

Appendix A

In this appendix we follow the guidelines of Beenaker (1986) to develop an efficient method for computing the flow due to a three-dimensional lattice of point-force dipoles and potential quadruples represented by the singularities $\mathscr{D}^{\mathrm{L}}$ and $\mathscr{Q}^{\mathrm{L}}$.

To compute $\mathscr{D}^{\mathrm{L}}$ we consider a single point-force dipole, $\mathscr{D}$, with pole at $\boldsymbol{X}$. Recalling that the point-force dipole is the derivative of the Green's function with respect to the pole, we write

$$\mathscr{D}(\boldsymbol{x}-\boldsymbol{X}) = \mathscr{D}^{(1)}(\boldsymbol{x}-\boldsymbol{X}) + \mathscr{D}^{(2)}(\boldsymbol{x}-\boldsymbol{X}), \tag{A 1}$$

where

$$\begin{bmatrix} \mathscr{D}^{(1)}_{jim} \\ \mathscr{D}^{(2)}_{jim} \end{bmatrix}(\boldsymbol{x}-\boldsymbol{X}) = -\left(\delta_{ji}\frac{\partial}{\partial x_m}\nabla^2 - \frac{\partial^3}{\partial x_j\,\partial x_i\,\partial x_m}\right)\begin{bmatrix} r\,\mathrm{erfc}\,(\xi r) \\ r\,\mathrm{erf}\,(\xi r) \end{bmatrix}, \tag{A 2}$$

$r = |\boldsymbol{x}-\boldsymbol{X}|$, and ξ is an arbitrary positive constant. After some algebra we find

$$\mathscr{D}^{(1)}_{jim}(\boldsymbol{x}) = \delta_{ji}\frac{x_m}{|\boldsymbol{x}|^3}F(\xi|\boldsymbol{x}|) - \frac{\delta_{mi}x_j + \delta_{mj}x_i}{|\boldsymbol{x}|^3}D(\xi|\boldsymbol{x}|) + \frac{x_j x_i x_k}{|\boldsymbol{x}|^5}E(\xi|\boldsymbol{x}|), \tag{A 3}$$

where

$$\begin{bmatrix} F \\ D \\ E \end{bmatrix}(x) = \mathrm{erfc}\,(x)\begin{bmatrix} 1 \\ 1 \\ 1 \end{bmatrix} + \frac{2}{\pi^{\frac{1}{2}}}x\exp(-x^2)\begin{bmatrix} 1-10x^2+4x^4 \\ 1-2x^2 \\ 3+2x^2-4x^4 \end{bmatrix}. \tag{A 4}$$

To obtain an array of point force dipoles we sum each term on the right-hand side of (A 4) over all lattice points $\boldsymbol{X}_l$. To compute the sum of $\mathscr{D}^{(2)}$, we introduce the reciprocal lattice base vectors defined as

$$\boldsymbol{b}_1 = \frac{2\pi}{\tau}\boldsymbol{a}_2 \times \boldsymbol{a}_3, \quad \boldsymbol{b}_2 = \frac{2\pi}{\tau}\boldsymbol{a}_3 \times \boldsymbol{a}_1, \quad \boldsymbol{b}_3 = \frac{2\pi}{\tau}\boldsymbol{a}_1 \times \boldsymbol{a}_2, \tag{A 5}$$

where τ is the volume of one cell, and construct the reciprocal lattice with vertices at the points

$$\boldsymbol{k}_\lambda = i_1\boldsymbol{b}_1 + i_2\boldsymbol{b}_2 + i_3\boldsymbol{b}_3, \tag{A 6}$$

where i_1, i_2, i_3 are integers. It is evident that the physical and reciprocal lattice vectors satisfy the equation $\boldsymbol{X}_l \cdot \boldsymbol{k}_\lambda = 2\pi m$, where m is an integer. Furthermore, we introduce the three-dimensional Fourier transform of a function $\boldsymbol{G}(\boldsymbol{x}-\boldsymbol{X})$ with respect to $\boldsymbol{X}$, defined as

$$\hat{\boldsymbol{G}}(\boldsymbol{k}, \boldsymbol{x}) = \int \exp(\mathrm{i}\boldsymbol{k}\cdot\boldsymbol{X})\, \boldsymbol{G}(\boldsymbol{x}-\boldsymbol{X})\, \mathrm{d}^3\boldsymbol{X}. \tag{A 7}$$

Using the three-dimensional version of the Poisson summation formula which stems from Parseval's formula (Nijboer & De Wette 1957), we obtain

$$\sum_{l=0}^{\infty} \boldsymbol{G}(\boldsymbol{x}-\boldsymbol{X}_l) = \frac{1}{\tau}\sum_{\lambda=0}^{\infty} \hat{\boldsymbol{G}}(\boldsymbol{k}_\lambda, \boldsymbol{x}). \tag{A 8}$$

Applying (A 8) with $\mathscr{D}^{(2)}$ in place of $\boldsymbol{G}$, and computing the Fourier transform in (A 7) working in spherical polar coordinates, we find

$$\sum_{l=0}^{\infty} \mathscr{D}^{(2)}_{jim}(\boldsymbol{x}-\boldsymbol{X}_l) = -\frac{8\pi}{\tau}\sum_{\lambda=1}^{\infty} \mathscr{F}_{jim}(\boldsymbol{x}, \boldsymbol{k}_\lambda), \tag{A 9}$$

where
$$\mathscr{F}_{jim}(\boldsymbol{x}, \boldsymbol{k}) = \sin(\boldsymbol{k}\cdot\boldsymbol{x})\frac{k_m}{|\boldsymbol{k}|^2}\left(\delta_{ji} - \frac{k_j k_i}{|\boldsymbol{k}|^2}\right)(1 + \tfrac{1}{4}\omega^2 + \tfrac{1}{8}\omega^4)\exp(-\tfrac{1}{4}\omega^2), \tag{A 10}$$

and $\omega = |\boldsymbol{k}|/\xi$. In summary, we find that the flow due to a lattice of point-force dipoles is given by

$$\mathscr{D}^{\mathrm{L}}(\boldsymbol{x}, \boldsymbol{X}) = \sum_{l=0}^{\infty} \mathscr{D}^{(1)}_{jim}(\boldsymbol{x}-\boldsymbol{X}_l) - \frac{8\pi}{\tau}\sum_{\lambda=1}^{\infty} \mathscr{F}_{jim}(\boldsymbol{x}, \boldsymbol{k}_\lambda). \tag{A 11}$$

Next, we consider the flow due to a lattice of potential quadruples expressed by $\mathscr{Q}^{\mathrm{L}}$. Using the relation $\mathscr{Q}^{\mathrm{L}} = -\frac{1}{2}\nabla^2\mathscr{D}^{\mathrm{L}}$ and differentiating (A 11) we find

$$\mathscr{Q}^{\mathrm{L}}(\boldsymbol{x}-\boldsymbol{X}) = \sum_{l=0}^{\infty} \mathscr{Q}^{(1)}(\boldsymbol{x}-\boldsymbol{X}_l) - \frac{4\pi}{\tau}\sum_{\lambda=1}^{\infty} |\boldsymbol{k}_\lambda|^2 \mathscr{F}(\boldsymbol{x}, \boldsymbol{k}_\lambda), \tag{A 12}$$

where
$$\mathscr{Q}^{(1)}_{jim}(\boldsymbol{x}) = -\delta_{ji}\frac{x_m}{|\boldsymbol{x}|^5}F(\xi|\boldsymbol{x}|) - 3\frac{\delta_{mi}x_j + \delta_{mj}x_i}{|\boldsymbol{x}|^5}K(\xi|\boldsymbol{x}|) + 3\frac{x_j x_i x_k}{|\boldsymbol{x}|^7}N(\xi|\boldsymbol{x}|), \tag{A 13}$$

with
$$\begin{bmatrix} M \\ K \\ N \end{bmatrix}(x) = \operatorname{erfc}(x)\begin{bmatrix} 3 \\ 1 \\ 5 \end{bmatrix} + \frac{2}{\pi^{\frac{1}{2}}}x\exp(-x^2)\begin{bmatrix} 3+2x^2+68x^4-56x^6+8x^8 \\ \frac{1}{3}(3+2x^2-16x^4+4x^6) \\ \frac{1}{3}(5+10x^2+4x^4-40x^6+8x^8) \end{bmatrix}. \tag{A 14}$$

Owing to the exponential decay of $\mathscr{D}^{(1)}$ and $\mathscr{Q}^{(1)}$, the first sums on the right-hand sides of (A 11) and (A 12) may be computed efficiently by direct summation. Owing

to the exponential decay of the function $\mathscr{F}$, the second sums may also be computed efficiently by direct summation. Adding the two sums yields a result which is independent of the value of ξ. Beenaker (1986) recommends using $\xi = \sqrt{2}/\tau^{\frac{1}{3}}$ for fastest convergence, and the success of this selection was confirmed in our computations. With this choice we find that, in most cases, summation over one or two or three lattice or reciprocal lattice layers is sufficient for accuracy extending up to the eighth decimal place.

Appendix B

The modified Green's function $\boldsymbol{G}^{\mathrm{M}}$ was developed by Brady *et al.* (1988) as a special case of the periodic Rotne–Prager tensor considered previously by Beenaker (1986). The derivation follows the steps outlined in Appendix A, and the result is

$$\boldsymbol{G}^{\mathrm{M}}(\boldsymbol{x}, \boldsymbol{X}) = \sum_{l=0}^{\infty} \boldsymbol{G}^{(1)}(\boldsymbol{x} - \boldsymbol{X}_l) + \frac{8\pi}{\tau} \sum_{\lambda=1}^{\infty} \mathscr{H}(\boldsymbol{x}, \boldsymbol{k}_\lambda), \tag{B 1}$$

where

$$G_{ij}^{(1)}(\boldsymbol{x}) = \frac{\delta_{ij}}{|\boldsymbol{x}|} C(\xi|\boldsymbol{x}|) + \frac{x_i x_j}{|\boldsymbol{x}|^3} D(\xi|\boldsymbol{x}|) \tag{B 2}$$

and

$$\mathscr{H}_{ij}(\boldsymbol{x}, \boldsymbol{k}) = \cos(\boldsymbol{k}\cdot\boldsymbol{x}) \frac{1}{|\boldsymbol{k}|^2} \left(\delta_{ji} - \frac{k_j k_i}{|\boldsymbol{k}|^2} \right) (1 + \tfrac{1}{4}\omega^2 + \tfrac{1}{8}\omega^4) \exp(-\tfrac{1}{4}\omega^2). \tag{B 3}$$

The function D is given in (A 4) and the function C is given by

$$C(x) = \operatorname{erfc}(x) + \frac{2}{\pi^{\frac{1}{2}}} (2x^2 - 3)\, x \exp(-x^2). \tag{B 4}$$

It will be noted that when $\xi = 0$, the first sum in (B 1) vanishes and the result is Hasimoto's (1959) fundamental solution representing an array of point forces.

REFERENCES

Ackerson, J. & Clark, N. A. 1983 Sheared colloidal suspensions. *Physica* **118A**, 221–249.

Acrivos, A. & Chang, E. Y. 1987 The transport properties of non-dilute suspensions. Renormalization via an effective continuum model. *AIP Conf. Proc. on Physics and Chemistry of Porous Media II*, vol. 154, pp. 129–142.

Adler, P. M. 1984 Spatially periodic suspensions of convex particles in linear shear flow. IV. Three-dimensional flow. *J. Méc. Théor. Appl.* **3**, 725–746.

Adler, P. M. & Brenner, H. 1985 Spatially periodic suspensions of convex particles in linear shear flows. I. Description and Kinematics. *Intl J. Multiphase Flow* **11**, 361–385.

Adler, P. M., Zuzovsky, M. & Brenner, H. 1985 Spatially periodic suspensions of convex particles in linear shear flows. II. Rheology. *Intl J. Multiphase Flow* **11**, 387–417.

Beenaker, C. W. J. 1986 Ewald sum of the Rotne–Prager tensor. *J. Chem. Phys.* **85**, 1581–1582.

Brady, J. F., Phillips, R. J., Lester, J. C. & Bossis, G. 1988 Dynamic simulation of hydrodynamically interacting suspensions. *J. Fluid Mech.* **195**, 257–280.

Edwards, D. A. & Wasan, D. T. 1991 A micromechanical model of linear surface rheological behavior. *Chem. Engng Sci.* **46**, 1247–1257.

Frankel, N. A. & Acrivos, A. 1967 On the viscosity of a concentrated suspension of solid spheres. *Chem. Engng Sci.* **22**, 847–853.

Hasimoto, H. 1959 On the periodic fundamental solutions of the Stokes equations and their application to viscous flow past a cubic array of spheres. *J. Fluid Mech.* **5**, 317–328.

Hinch, E. J. 1991 *Perturbation Methods*. Cambridge University Press.

HOFFMAN, R. L. 1972 Discontinuous and dilatant viscosity behavior in concentrated suspensions I. Observation of a flow instability. *Trans. Soc. Rheol.* **16**, 155–173.

HOFFMAN, R. L. 1974 Discontinuous and dilatant viscosity behavior in concentrated suspensions II. Theory and Experimental Tests. *J. Colloid Interface Sci.* **46**, 491–506.

HURD, A. J., CLARK, N. A., MOCKLER, R. C. & O'SULLIVAN, W. J. 1985 Friction factors for a lattice of Brownian particles. *J. Fluid Mech.* **153**, 401–416.

KAPRAL, R. & BEDEAUX, D. 1978 The effective shear viscosity of a regular array of suspended spheres. *Physica* **91A**, 590–602.

KIM, S. & LU, S.-Y. 1987 The functional similarity between Faxén relations and singularity solutions for fluid–fluid, fluid–solid and solid–solid dispersions. *Intl J. Multiphase Flow* **13**, 837–844.

LONGUET-HIGGINS, M. S. & COKELET, E. D. 1976 The deformation of steep surface waves on water I. A numerical method of computation. *Proc. R. Soc. Lond.* A **350**, 1–26.

MARRUCCI, G. & DENN, M. M. 1985 On the viscosity of a concentrated suspension of solid spheres. *Rheol. Acta* **24**, 317–320.

NIJBOER, B. R. A. & DE WETTE, F. W. 1957 On the calculation of lattice sums. *Physica* **23**, 309–321.

NITSCHE, L. C. & BRENNER, H. 1989 Eulerian kinematics of flow through spatially periodic models of porous media. *Arch. Rat. Mech.* **107**, 225–292.

NUNAN, K. C. & KELLER, J. B. 1984 Effective viscosity of a periodic suspension. *J. Fluid Mech.* **142**, 269–287.

PHAN-THIEN, N., TRAN-CONG, T. & GRAHAM, A. L. 1991 Shear flow of periodic arrays of particle clusters: a boundary-element method. *J. Fluid Mech.* **228**, 275–293.

POZRIKIDIS, C. 1992 *Boundary Integral and Singularity Methods for Linearized Viscous Flow.* Cambridge University Press.

RALLISON, J. M. 1978 Note on the Faxén relations for a particle in Stokes flow. *J. Fluid Mech.* **88**, 529–533.

RALLISON, J. M. 1984 The deformation of small viscous drops and bubbles in shear flows. *Ann. Rev. Fluid Mech.* **16**, 45–66.

SAFFMAN, P. G. 1973 On the settling speed of free and fixed suspensions. *Stud. Appl. Maths* **52**, 115–127.

SANGANI, A. S. 1987 Sedimentation in ordered emulsions of drops at low Reynolds numbers. *Z. Angew. Math. Phys.* **38**, 542–556.

SANGANI, A. S. & ACRIVOS, A. 1982 Slow flow through a periodic array of spheres. *Intl J. Multiphase Flow* **8**, 343–360.

SANGANI, A. S. & LU, W. 1987 Effective viscosity of an ordered suspension of small drops. *Z. Angew. Math. Phys.* **38**, 557–572.

SECOMB, T. W., FISCHER, T. M. & SKALAK, R. 1983 The motion of close-packed red blood cells in shear flow. *Biorheol.* **20**, 283–294.

TAYLOR, G. I. 1932 The viscosity of a fluid containing small drops of another fluid. *Proc. R. Soc. Lond.* A **138**, 41–48.

TAYLOR, G. I. 1934 The formation of emulsions in definable fields of flow. *Proc. R. Soc. Lond.* A **146**, 501–523.

THOMAS, D. G. 1965 Transport characteristics of suspensions: VIII. A note on the viscosity of Newtonian suspensions of uniform spherical particles. *J. Colloid Sci.* **20**, 267–277.

WANG, M. L. & CHEAU, T.-C. 1990 Singular behavior of the effective viscosity in a concentrated suspension medium. *Chem. Engng Commun.* **87**, 143–161.

ZICK, A. A. & HOMSY, G. M. 1982 Stokes flow through periodic arrays of spheres. *J. Fluid Mech.* **115**, 13–26.

ZUZOVSKY, M., ADLER, P. M. & BRENNER, H. 1983 Spatially periodic suspensions of convex particles in linear shear flows. III. Dilute arrays of spheres suspended in Newtonian fluids. *Phys. Fluids* **26**, 1714–1723.